The Modulatory Site for the Action of Gadolinium on Surface Charges and Channel Gating

Fredrik Elinder and Peter Århem
The Nobel Institute for Neurophysiology, Karolinska Institutet, S-171 77 Stockholm, Sweden

ABSTRACT The gadolinium (Gd^{3+})-induced shift of potential dependence and modulated gating of Na and K channels were analyzed. In a previous investigation, we explained the shift in terms of pure screening (no binding) of fixed surface charges and the modulation by binding to modulatory sites on the channels. In the present paper, we have extended this model by including effects on the charge density of Gd^{3+} binding to the modulatory sites. From fitting the extended model to experimental data, the charge density was estimated to be -0.6 e nm^{-2}, and the Gd^{3+}-induced charge change to be $+0.15$ e nm^{-2}, and the maximal scaling factor to be 7.5 for both Na and K channels. Intrinsic K_D values for binding to the K and Na channels were estimated to be 140 and 380 mM, respectively. Estimations of the extracellular charge density, from primary structures of cloned channels, were found to be in agreement with estimations based on the present model. The modulatory site was suggested to be located at the cluster of negatively charged residues between the fifth transmembrane segment (S5) and the pore-forming region for both Na and K channels. These suggestions imply several testable predictions about different K channels.

INTRODUCTION

In the preceding paper, we described the effects of the trivalent gadolinium ion (Gd^{3+}) on Na, K, and leakage currents in myelinated amphibian axons (Elinder and Århem, 1994). The effects were tentatively interpreted in terms of Gd^{3+} action on four different sites: (i) screening of fixed surface charges, causing a modified surface potential according to the Gouy-Chapman theory, (ii) binding to a modulatory site on both Na and K channels, causing a slowed rate of gating, quantified as a scaling of time constant curves by a factor A, (iii) binding to a blocking site on both Na and K channels, and (iv) binding to a site at the interface between channels and the lipid phase, causing block of the leakage current.

In the present paper, we will discuss the screening effect and the binding to modulatory sites. Both theoretical reasons and experimental data suggest that the effective fraction of the fixed surface charges is located on the channels. The estimated Debye length in Ringer solution is 0.9 nm, which is short in relation to the channel dimensions. Enzymatic removal of sialic acid residues (Frankenhaeuser et al., 1976; Ohmori and Yoshii, 1977) and changed composition of lipid bilayers (Bell and Miller, 1984; Green et al., 1987; Cukierman et al., 1988; Worley et al., 1992) seem to have negligible effects on potential dependent channel parameters (but see Recio-Pinto et al., 1990). Thus, binding of a Gd^{3+} ion to a modulatory site located on the channel is expected to affect the effective fraction of the fixed surface charges and interfere with the screening effect. The aim of the present study was to explore quantitatively a model that takes this into account. With such a model, we have improved the estimation of the surface charge density of the previous investigation, and we have obtained values for the intrinsic dissociation constants for Gd^{3+} binding to the modulatory site of Na and K channels. The results are discussed in relation to recent electrophysiological and structural data (Armstrong and Cota, 1990; Durell and Guy, 1992), and some testable predictions are proposed.

MATERIALS AND METHODS

Experimental data

The experimental data forming the basis for the computations are described in the previous paper (Elinder and Århem, 1994).

Quantitative treatment

The quantitative treatment was based on the following basic assumptions:
(i) Gd^{3+} is reversibly bound to the modulatory site in a one-to-one manner according to

$$y = 1/(1 + K_D/[Gd^{3+}]_0), \quad (1)$$

where y is the fractional occupancy, K_D is the intrinsic dissociation constant for the binding, and $[Gd^{3+}]_0$ is the surface concentration of Gd^{3+}.
(ii) The surface concentration is related to the bulk concentration ($[Gd^{3+}]$) by a Boltzmann relation

$$[Gd^{3+}]_0 = [Gd^{3+}]\exp(-3F\psi_0/(RT)), \quad (2)$$

where ψ_0 is the surface potential minus the bulk potential. R, T, and F have their usual meanings.
(iii) The surface potential is related to the free surface charge density (σ) by the Grahame equation (modification of Eq. 40 in Grahame, 1947)

$$\sigma^2 = 2\epsilon\epsilon_0 RT \sum_i c_i \left(\exp\left(-\frac{z_i F\psi_0}{RT}\right) - 1\right), \quad (3)$$

where c_i is the bulk concentration, and z_i is the valence of the ith ionic species. ϵ and ϵ_0 are the dielectric constants of the medium and the permittivity of free space and have the values 78 and 8.85×10^{-12} Fm^{-1}. Although Eq. 3 is strictly valid only for a uniformly smeared charge, we will use it as an approximation for the present case with discrete charges (see McLaughlin, 1989). The concentrations used for calculation of Eq. 3 (see Results) are described in the preceding paper (Elinder and Århem, 1994).

Received for publication 16 August 1993 and in final form 22 April 1994.
Address reprint requests to Peter Århem, Karolinska Institutet, The Nobel Institute for Neurophysiology, S-17177 Stockholm, Sweden. Tel. 011-46-8-728-64-03; Fax: 011-46-8-34-95-44.

0006-3495/94/07/84/07 $2.00

The theory of absolute reaction rates (Glasstone et al., 1941) was used in the discussion of the Gd^{3+} effects on the rate constants of the channel kinetics. The equation used assumes one barrier and is described by

$$\alpha = kT/h \exp(-(W_0 + zeU)/(kT)), \quad (4)$$

where α is the forward rate constants for the Na or the K channel (as defined in the previous paper), k is the Boltzmann constant, h is the Planck constant, W_0 is the activation energy (well to activation peak) at a membrane potential (U) of 0, z is the gating charge, and e is the charge of an electron. The same equation may be used for the corresponding backward rate constants (β).

The computations were made on a personal computer (CPU 80486), and the programs were written in BASIC.

RESULTS

Theory

The specific aim of this section is to develop equations that relate the observed scaling factors A and the shifts $\Delta U_{1/2}$ of the preceding paper (Elinder and Århem, 1994) to the binding of Gd^{3+} to the modulatory site. The derivations were based on the assumption of separate blocking and modulatory sites (see Elinder and Århem, 1994). This means that the following discussion concerns exclusively the fraction of unblocked channels. The derived equations will be used to quantify properties of the channels, such as the binding constant (K_D), the surface charge density (σ) and the change in surface charge density caused by Gd^{3+} binding ($\Delta\sigma^*$). Note that A in the following denotes the scaling factor after correction for the inactivation effect (i.e., it is equal to A^* of the preceding paper).

Scaling of time constant curves

Let us for simplicity assume that the opening of the channels (described by permeability $P(t)$) in Ringer solution follows the monoexponential equation

$$P(t) = 1 - \exp(-t/\tau) = 1 - 2^{-t/t_{1/2}}. \quad (5a)$$

At the concentration where A has reached its maximum (A_{max}), the opening is described by

$$P^*(t) = 1 - \exp(-t/(A_{max}\,\tau)) = 1 - 2^{-t/(A_{max}t_{1/2})}. \quad (5b)$$

At this concentration, all channels are bound all the time. At lower concentrations, the opening process can be more complex. This depends on the rate of binding/unbinding to the modulatory site. Here we assume that the rate is infinitely slow. This applies to the case when the binding/unbinding is slow compared to the time scale used in the experiments, that is, when a Gd^{3+} ion is bound to the modulatory site it remains bound during the potential step and vice versa. The case of an infinitely fast rate is treated in the Appendix. The results obtained for both of these extreme cases were qualitatively similar, but the derivation assuming an infinitely slow rate showed a better fit to experimental data than did the case of an infinitely fast rate (see below). In the present case, we thus assume that at a given Gd^{3+} concentration, the fraction y are bound channels and $1 - y$ are unbound. The opening is here described by

$$P_{mix}(t) = y(1 - 2^{-t/(A_{max}t_{1/2})}) + (1 - y)(1 - 2^{-t/t_{1/2}}). \quad (6)$$

By definition $P_{mix}(t) = 0.5$ at $t = At_{1/2}$ and we obtain

$$y = (2^{-A} - 2^{-1})/(2^{-A} - 2^{-A/A_{max}}). \quad (7)$$

Shift of activation curves

The steady-state activation (and inactivation) curves in control solution can approximately be described by the Boltzmann distribution

$$P(U) = 1/(1 + \exp((U_{1/2} - U)/k)), \quad (8)$$

where $P(U)$ is normalized permeability, $U_{1/2}$ is the potential at $P = 0.5$, U is the membrane potential, and k is the slope constant (i.e., 6.0 mV for Na activation, −8.0 for Na inactivation and 9.0 for K activation; see Elinder and Århem, 1994). In test solution, the corresponding curves can be described by

$$P_{mix}(U) = 1/(1 + \exp((U_{1/2} + \Delta U_{1/2} - U)/k_{mix})), \quad (9)$$

where $\Delta U_{½}$ is the experimentally obtained shift, and k_{mix} is the slope constant. Under these conditions, a fraction y of the channels is assumed to be bound, and the charge density of the channels changed from σ to $\sigma + \Delta\sigma^*$. A fraction $1 - y$ of the channels is assumed to be unbound. For the total population channels in test solution, we thus obtain

$$P_{mix}(U) = (1 - y)\,(1/(1 + \exp((U_{1/2} + \Delta\psi_0 - U)/k))) + y\,(1/(1 + \exp((U_{1/2} + \Delta\psi_0^* - U)/k))), \quad (10)$$

where $\Delta\psi_0$ and $\Delta\psi_0^*$ are changes in channel surface potential when control solution is changed to test solution in the unbound and bound case, respectively. This curve can be fitted by a nonlinear least-square procedure to the experimentally obtained curve described by Eq. 9 above. For sufficiently small $|\Delta\psi_0 - \Delta\psi_0^*|$, the nonlinear relation between $\Delta U_{1/2}$ and y (from the combination of Eqs. 9 and 10) could be linearized to

$$\Delta U_{1/2} = (1 - y)\Delta\psi_0 + y\Delta\psi_0^* \quad (11)$$

Numerical tests showed that $|\Delta\psi_0 - \Delta\psi_0^*| < |3k|$ gave an error less than 0.05 k and Eq. 11 was therefore used in the following calculations.

Comparison with experimental data

The derived equations were used to determine the parameters σ, K_D, A_{max}, and $\Delta\sigma^*$. This was done in two steps. First, we fitted an A vs. $[Gd^{3+}]$ curve to the data of Fig. 1. For this we did not need the $\Delta\sigma^*$ value, because only the binding to the modulatory site and not the unbinding is concentration-dependent. (Gd^{3+} binds per definition to unbound channels, where the charge density is σ, and unbinds from bound channels, where the charge density is $\sigma + \Delta\sigma^*$). Thus, in this step we only have three unknown parameters to determine. By fixing a σ value, we can easily calculate K_D and A_{max} from Eqs. 1–3 and 7 by a least-square procedure. Under these conditions, K_D determines the position of the curve on the concentration axis and A_{max} the height. We determined K_D

and A_{max} values for σ values in the range given in Hille et al. (1975). Fig. 1 shows the least-square fitted A vs. $[Gd^{3+}]$ curves for both K and Na channels at the charge densities -0.4 and -1.0 e nm^{-2}. The K_D and A_{max} values obtained are given in Table 1. The fit was slightly better for the -0.4 e nm^{-2} than for the -1.0 e nm^{-2} curve.

In the second step, we used the values of σ, K_D, and A_{max} from above to fit $\Delta U_{1/2}$ vs. $[Gd^{3+}]$ curves to the data. This procedure left only parameter $\Delta\sigma^*$ to be determined. This was done for $[Gd^{3+}] = 100$ μM at different surface charge densities by using $\Delta U_{1/2} = 9$ mV (from Fig. 2) and Eqs. 1–3, 7, and 11. We then calculated $\Delta U_{1/2}$ for other concentrations. Fig. 2 shows the $\Delta U_{1/2}$ vs. $[Gd^{3+}]$ relation for the Na system, calculated for the charge densities -0.4 and -1.0 e nm^{-2}. Associated parameters are shown in Table 1. At the higher concentration range, calculations for -0.6 e nm^{-2} are also included (*dashed line*). As seen, the fit is slightly better for values more negative than -0.6 e nm^{-2} than for values more positive.

Table 1 shows values for the calculated parameters at four different surface charge densities. Comparing the results from the two fitting procedures above suggests that the best fit is obtained for a surface charge density of about -0.6 e nm^{-2}, and consequently for $K_D = 140$ μM, $A_{max} = 7.7$ and $\Delta\sigma^* = 0.13$ e nm^{-2} for the K channel and $K_D = 380$ μM, $A_{max} = 7.3$ and $\Delta\sigma^* = 0.16$ e nm^{-2} for the Na channel. An interesting observation, illustrated in Table 1, was the relative independence of $\Delta\sigma^*$ on the surface charge density; for σ values between -1.0 and -0.4 e nm^{-2} it varied between 0.09 and 0.13 e nm^{-2} for K channels, and between 0.13 and 0.17 e nm^{-2} for Na channels.

As mentioned above, the equations used assumed infinitely slow binding/unbinding. Quantitatively similar results were obtained by assuming infinitely fast binding/unbinding (see Appendix), the corresponding K_D values being about 50% smaller, and A_{max} values larger.

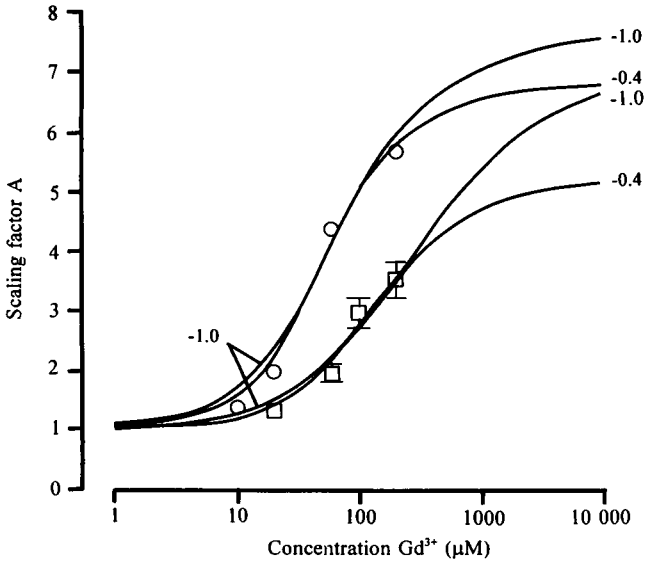

FIGURE 1 Relation between the scaling factor A and Gd^{3+} concentration for both K (○) and Na (□) channels. Bars indicate the highest and lowest values obtained (from Elinder and Århem. 1994). The curves are solutions to the model described in the text (least-square fitted to experimental data) for different surface charge densities as indicated (e nm^{-2}).

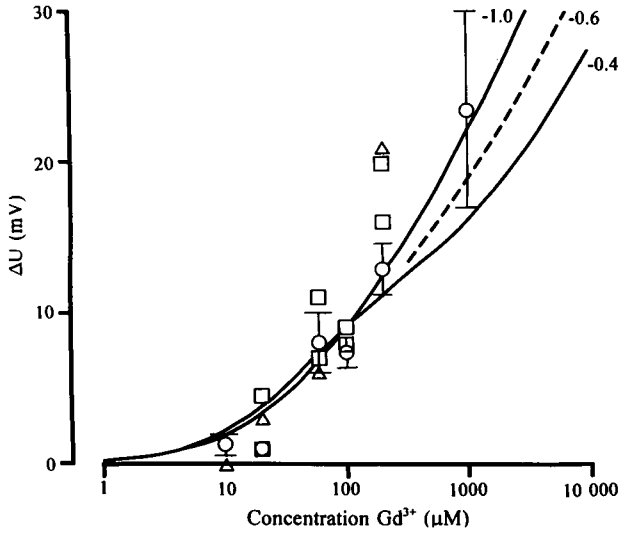

FIGURE 2 Relation between potential shift (ΔU) and Gd^{3+} concentration. The symbols indicate shifts of activation and inactivation curves for Na channels (○, mean ± SEM), and shifts of time constant curves for Na (□, highest and lowest values) and K (Δ) channels (from Elinder and Århem, 1994). The curves are solutions for the model described in the text for different surface charge densities as indicated (e nm^{-2}).

TABLE 1 Least-square fitted values to data points in Figs. 2 and 3 for different surface charge densities

	K			Na		
σ (e nm^{-2})	K_D (mM)	A_{max}	$\Delta\sigma^*$ (e nm^{-2})	K_D (mM)	A_{max}	$\Delta\sigma^*$ (e nm^{-2})
−0.4	25	7.1	0.10	62	5.7	0.13
−0.6	140	7.7	0.13	380	7.3	0.16
−0.8	480	8.5	0.13	1200	9.9	0.17
−1.0	1200	9.8	0.09	3000	13.5	0.13

Effect on activation curve slope

The model also predicts a changed slope of the activation curves. Using the estimated σ and $\Delta\sigma^*$ values (-0.6 and $+0.16$ e nm^{-2}), a surface potential difference ($\Delta\psi_0^* - \Delta\psi_0$) of about 10 mV (9.9–11.5 mV) at $[Gd^{3+}] < 100$ μM is obtained, yielding a maximal slope reduction (which occurs when 50% of the channel population is bound) for Na activation (at 70 μM Gd^{3+}) of about 12%, for Na inactivation about 8%, and for K activation (at about 50 μM Gd^{3+}) less than 6%. In the preceding paper, the relatively large slope reduction (17%) of the Na activation curve at 200 μM Gd^{3+} was possible to explain in terms of an inactivation effect. The present model might explain part of this effect but might, in addition, explain slope reductions observed for cases when inactivation is experimentally removed, such as that described by Armstrong and Cota (1990) for papain-treated

GH3 cells. These types of effect have also been discussed by Attwell and Eisner (1978).

DISCUSSION

In summary, we have developed a quantitative model based on elementary physicochemical principles, describing the Gd^{3+} effects on the gating and the surface potential by binding to a modulatory site. From fitting the model to experimental data of the previous investigation, we estimated that the charge density (σ) was -0.6 e nm^{-2}, the change in charge density due to the binding ($\Delta\sigma^*$) about 0.15 e nm^{-2} and the maximal scaling value (A_{max}) about 7.5 for both Na and K channels of the nodal membrane. The intrinsic dissociation constant (K_D) for the K channel was 140 mM and for the Na channel 380 mM. In the following section, we will extend the model by taking recent data from molecular studies of the channels into account, thereby increasing the predictive power of the model.

Surface charge density

As mentioned in the Introduction, there are strong indications that the effective surface charges are located on the channel protein. Therefore, we estimated the charge density of the predicted external portions of some known Na and K channels (Table 2). The estimation was based on the number of charges of the segments between S1 and S2, S3 and S4, and S5 and S6 (excepting the pore-forming P-segment, nomenclature of Stevens, 1991) (Guy and Conti, 1990; Miller, 1991; Miller, 1992). For K channels, the P-segment was defined as the 19 amino acid residues between the two prolines in accordance with Miller (1991). For the Na channel, the P-segments of the four domains were defined as corresponding stretches of 17 to 19 residues between two negatively charged residues, with the TTX binding sites (Terlau et al., 1991) at its C-terminal end in accordance with Miller (1992). The negatively charged residues at both ends of these segments were assumed here to belong to the extracellular portion, thus contributing to the surface charges. As seen from Table 2, the total net extracellular charge of Na channels varied from -23 to -15.5 e, whereas that of the K channels varied from -36 to $+6$ e.

The primary structures of the ion channels in the myelinated axon of *Xenopus laevis* are not yet known. It has been proposed that about two-thirds of the K channels in amphibian (Jonas et al., 1992) and rat (Safronov et al., 1993) axonal membrane are of the RCK1 type (=K_v1.1). This proposal is mainly based on kinetic and pharmacological studies. It correlates well with a high level of expressed mRNA of RCK1 in the rat sciatic nerve (Beckh and Pongs, 1990). The second type of fast K channel in amphibian axonal membrane has been proposed (Jonas et al., 1992) to be of Raw3 or Raw2 type (=K_v3.4 or K_v3.1). The Na channel has been studied in less detail. However, it has been shown that RBNa II channels preferentially are localized in axons, whereas types I and III are localized on neuronal cell bodies in vivo (Westenbroek et al., 1989; Numann et al., 1991).

To calculate the charge density of these channels, we assumed an extracellular area of 28 nm^2 ($\varnothing$ = 6 nm if lipid membrane thickness is 3 nm, measured from Durell and Guy, 1992). For RBNa II channels, we then obtain a value of -0.81 e nm^{-2}, in good agreement with the estimations from our experimental data (-0.6 e nm^{-2}). For RCK1 and Raw3 channels, we obtain values of -1.13 and $+0.21$ e nm^{-2}, respectively. Assuming that the population of K channels of the nodal membrane consists of a combination of these two types, the agreement with the estimation from our experimental data (-0.6 e nm^{-2}) is reasonable.

Therefore, we tentatively propose that the effective surface charge of a channel is closely correlated with the sum of charges of its extracellelarly located amino acids. This hypothesis implies a testable prediction. The screening effect of cations should differ for different channels. For instance, the effect on *Shaker* type (K_v1) channels should be much more pronounced than that on *Shab*, *Shaw*, or *Shal* type (K_v2,

TABLE 2 Extracellularly located charged residues of rat Na and K channels

		S1-S2	S3-S4	S5-S6	Total	Ref
	RBNa I	−4.5	−3	−10.5	−18	Noda et al. (1986)
⇒	RBNa II	−5.5	−2	−15.5	−23	Noda et al. (1986)
	RBNa III	−2.5	−3	−10	−15.5	Kayano et al. (1988)
⇒	RCK1 (K_v1.1)	−14	−8	−10	−32	Stühmer et al. (1989)
	RCK2 (K_v1.6)	−30	+6	−12	−36	Grupe et al. (1990)
	RCK3 (K_v1.3)	−24	0	−8	−32	Stühmer et al. (1989)
	RCK4 (K_v1.4)	−14	0	−6	−20	Stühmer et al. (1989)
	RCK5 (K_v1.2)	−16	−2	−8	−26	Stühmer et al. (1989)
	DRK1 (K_v2.1)	−16	+12	0	−4	Frech et al. (1989)
	cdrk (K_v2.2)	−12	+12	0	0	Hwang et al. (1992)
	Raw1 (K_v3.2)	−14	+4	−2	−12	Rettig et al. (1992)
(⇒)	Raw2 (K_v3.1)	−6	+4	0	−2	Rettig et al. (1992)
⇒	Raw3 (K_v3.4)	−4	+4	+6	+6	Rettig et al. (1992)
	MR*Shal* (K_v4.1)	−2	−8	+12	+2	Baldwin et al. (1991)

The definition of the used segments is described in the text. Glutamate and aspartate amino acids were assigned a charge of -1, arginines and lysines a charge of $+1$, and histidines a charge of $+0.5$. Proposed standard nomenclature (Chandy, 1991, Pongs, 1992) within parentheses. Channel types in the amphibian node (see text and Jonas et al., 1992) indicated by arrows. Values for K channels are calculated for four subunits.

K_v3, or K_v4) channels (see Table 2). This was corroborated in a preliminary analysis of Gd^{3+} and Mg^{2+} effects on the two populations nodal K channels (Elinder and Århem, 1993), separated by the method of Dubois (1981). The shift of the permeability curve for the RCK1 population was larger than that for the Raw3 population. Furthermore, the assumption of an extracellular area of 28 nm^{-2} predicts a change of charge density with 0.11 e nm^{-2} when a Gd^{3+} ion is bound to a modulatory site of the channel (assuming a uniformly smeared charge). This should be compared with the experimentally estimated values, 0.16 e nm^{-2} for the Na channel and 0.13 e nm^{-2} for the K channel (see Table 1).

The present calculations of the extracellular charges of different channel types (Table 2) also reveal a correlation between the sum of charges and the location of the activation curve on the voltage axis. The more negative the charge sum is, the more negative the midpoint of the activation curve becomes. The midpoint-value of *Shaker* type (K_v1) channels is -26 ± 7 mV (mean $\pm$ SD, $n = 5$; from Stühmer et al., 1989; Grupe et al., 1990), whereas that of Shaw type (K_v3) channels is $+7 \pm 11$ mV (n = 3; from Rettig et al., 1992). The corresponding charge sums are -29 ± 6 e and -3 ± 9 e, respectively (values from Table 2). However, it should be noted that the activation curve can also be shifted by point mutations not affecting the extracellular residues (i.e., an electroneutral mutation in the S4-segment (R371K) of a *Shaker* channel can shift the activation curve +60 mV; Papazian et al, 1991).

The location of the modulatory site

Concerning the location of the modulatory site on the channels, no data from site-directed mutagenesis are available at present. By analyzing the primary structure it is possible, however, to make some testable predictions. It is known that lanthanides in general show a preference for binding to O donor atoms (interaction with N or S would quickly be hydrolyzed), and the dominating O donor in proteins are the carboxyl groups of aspartate or glutamate residues (Evans, 1990). Other residues, such as cysteine and histidine, known to bind IIB ions, can be excluded as binding sites, because the Gd^{3+} effect on Na and K channels is both qualitatively and quantitatively similar, whereas the extracellular cysteine/histidine content of RBNa II and RCK1 differs considerably (7 histidine and 12 cysteine residues versus 2 and 0, respectively). (See also Spires and Begenisich, 1992b). We suggest, therefore, (i) that the modulatory Gd^{3+} binding site consists of aspartate and/or glutamate residues; we further suggest (ii) that it consists of a cluster of these negative residues, because of the trivalency of the Gd^{3+} ion; we also suggest (iii) that the modulatory site is located topologically close to the potential sensitive S4 segment, which seems to protrude into the extracellular space at depolarization (Pusch, 1990; Sammar et al., 1992); finally, we suggest (iv) that the modulatory site is located on a segment that is relatively short (<15 residues), and, thus, is in a relatively fixed position.

K channels

Atomic scale pictures of the *Shaker* A channel (Durell and Guy, 1992), assumed to be similar to the RCK1 channel, suggest that the most likely site is on the S5-P segment (see Fig. 3): (a) it is in close contact with the S4 segment, (b) it contains a cluster of four negative residues, and (c) the first of these residues (glutamate; *arrow* in Fig. 3) is conserved in all documented voltage-gated K channels and assumed to interact with the S4 segment (Durell and Guy, 1992; note, however, that this reference locates this particular residue within S5). The S1–S2 segment is longer (34 residues) and is located at some distance from the S4 segment. Further, a comparative analysis of different RCK channels suggests that it does not influence the channel properties (Grupe et al., 1990; see also Spires and Begenisich, 1992a). The S3–S4 segment seems for mechanical reasons unlikely to interfere with the S4 movement. Further, only a single negative residue is located in the vicinity of S4. We suggest, therefore, that Gd^{3+} binds to the RCK1 channel somewhere at the cluster of negatively charged residues of the S5-P segment. This suggestion implies a prediction: the Raw3 channel shows a different charge pattern for the S5-P segment; the negatively charged residues are intermingled with positively charged residues. Thus, we predict that Gd^{3+} (and other polyvalent cations) will affect Raw3 channels less than RCK1 channels.

Na-channels

Using the criteria discussed above and assuming a similar three-dimensional structure for the RBNa II channel as for the *Shaker* channel, we suggest that Gd^{3+} binds to the cluster of negative residues of the S5-P segment of domain IV. Binding to a similar cluster of the P-S6 segment in domain II was excluded since it contains a site for TTX, suggesting that

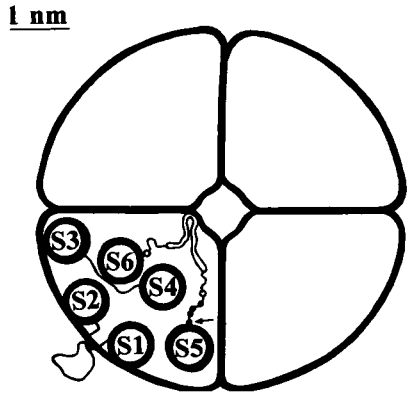

FIGURE 3 A schematic picture of the (*Shaker*) K channel viewed from the extracellular side (after Durell and Guy, 1992). Transmembranal segments (S1–S6) and extracellular linking segments are indicated in one of the four subunits. The pore-forming region is indicated with a double-lined segment (between S5 and S6). In this extracellular segment, negatively (●) and positively (○) charged amino acid residues (in the RCK1 channel) are also indicated. The arrow indicates a residue conserved for all known K channels, which is assumed to interact with the S4 segment (Durell and Guy, 1992).

Gd^{3+} binding here would block the channel. We can, on the other hand, add the two conserved aspartate residues of the P-S6 segment of domain IV, proposed to interact with positive charges of the S4 segment (Trimmer et al. (1989) and references within), as a possible binding site.

Number of binding sites

The model discussed is based upon the assumption of one modulatory site per channel. One reason for this was the predicted reduction in probability of binding when a Gd^{3+} is bound to the site, because of the reduction of Gd^{3+} concentration at the membrane surface. At 100 μM [Gd^{3+}], the surface concentration at unbound Na channels ($\sigma = -0.6$ e nm^{-2}) is predicted to 490 mM Gd^{3+} (Eqs. 2 and 3), whereas at channels with one bound Gd^{3+} ($\sigma = -0.6 + 0.16 = -0.44$ e nm^{-2}) to 140 mM, implying a reduced probability of binding by a factor of 3.5. Such a dynamic Gd^{3+} binding to channels will also modify pH at the surface. However, this modification should be less than 0.2 pH units, and was neglected in our calculations.

The scaling effect of divalent and monovalent ions

The present model can also be used to predict scaling effects of divalent and monovalent ions on the rate constants (or time constants) of the Na and K channels (Elinder and Århem, 1994). Expressing the rate constants in terms of the theory of absolute reaction rates (see Materials and Methods; Eq. 4) we obtain for a bound channel,

$$\alpha/A_{max} = kT/h \exp(-(W_0 + \Delta W + zeU)/(kT)), \quad (12)$$

where α denotes the forward activation rate constant of an unbound channel and ΔW the increase in activation peak produced by Gd^{3+} binding to the modulatory site. This yields

$$\Delta W = kT \ln A_{max}. \quad (13)$$

Assuming an A_{max} value of 7.5, we obtain $\Delta W = 2.0\,kT$ (=4.7 kJ/mol at 8°C; about a tenth of the total activation energy). Assuming further that a monovalent cation induces a barrier of $1/3\Delta W$ when bound, and a divalent cation a barrier of $2/3\Delta W$, A_{max} values of 2.0 and 3.8 for these ions are predicted. The highest A value for a divalent cation calculated from reported data in the literature is 3.3 (for Zn^{2+}, from Århem, 1980; see Discussion in the preceding paper).

CONCLUSION

In conclusion, by comparing the model for the modulatory action of Gd^{3+} on gating and surface charges with the experimental data of the previous investigation (Elinder and Århem, 1994), we could estimate σ, $\Delta\sigma^*$, A_{max}, and K_D for the nodal Na and K channels. By taking data from studies on the molecular structure of channels into account, and by making the assumptions that (a) the extracellular segments contain essentially the fixed surface charges, and that (b) Gd^{3+} binds to critical portions of the extracellular segments (due to criteria discussed above), we could extend the model to include the possible binding sites for Gd^{3+} on the nodal Na and K channels. From this extended model, we could make the following testable predictions: (1) The screening effect of Gd^{3+} and other cations will be larger on *Shaker* type channels (including RCK1) than on *Shaw* (including Raw3), *Shab*, or *Shal* type channels; (2) The modulatory effect of Gd^{3+} and other cations will be larger on RCK1 than on Raw3 channels; and (3) The modulatory effect per channel expressed in A_{max} will be about 3.8 for divalent cations and about 2.0 for monovalent cations. The first prediction has been corroborated in preliminary experiments (Elinder and Århem, 1993).

We thank Dr. Russell Hill, Department of Neuroscience at Karolinska Institute, for valuable comments on the manuscript.
This work was supported by grants from the Swedish Medical Research Council (project No 6552), The Karolinska Institute, and the Swedish Society for Medical Research.

APPENDIX

The scaling factor at fast binding and unbinding

In this section, we derive the equation relating the fractional occupancy y to the A value for the case of infinitely fast Gd^{3+} binding/unbinding to the modulatory site. In this case, y denotes the fraction of any given time interval the channel is bound, and consequently $1 - y$ denotes the time fraction when the channel is unbound. For simplicity we assume, as in the case of infinitely slow binding/unbinding above, a monoexponential time course for the control case. Thus, we obtain an opening time course in control solution as described by Eq. 5a, and in a test solution in which A reaches its maximum value (A_{max}), and consequently all channels are bound all the time, as described by Eq. 5b. At lower Gd^{3+} concentrations, the opening time course (for permeability $P_{mix}(t)$) is described by

$$P_{mix}(t) = 1 - 2^{-t((1-y)/t_{1/2} + y/(A_{max}t_{1/2}))}. \quad (A1)$$

By definition, $P_{mix}(t) = 0.5$ at $t = At_{1/2}$ and we obtain

$$0.5 = 2^{-A((1-y) + y/A_{max})}$$

and consequently

$$y = (A_{max}/A - A_{max})/(1 - A_{max}). \quad (A2)$$

REFERENCES

Århem, P. 1980. Effects of some heavy metal ions on the ionic currents of myelinated fibres from *Xenopus laevis J. Physiol.* 306:219–231.

Armstrong, C. M., and G. Cota. 1990. Modification of sodium channel gating by lanthanum. *J. Gen. Physiol.* 96:1129–1140.

Attwell, D., and Eisner, D. 1978. Discrete membrane surface charge distributions. *Biophys. J.* 24:869–875.

Baldwin, T. J., M.-L. Tsaur, G. A. Lopez, Y. N. Jan, and L. Y. Jan. 1991. Characterization of a mammalian cDNA for an inactivating voltage-sensitive K^+ channel. *Neuron.* 7:471–483.

Beckh, S., and O. Pongs. 1990. Members of the RCK potassium channel family are differentially expressed in the rat nervous system. *EMBO J.* 9:777–782.

Bell, J. E., and C. Miller. 1984. Effects of phospholipid surface charge on ion conduction in the K^+ channel of sarcoplasmic reticulum. *Biophys J.* 45:279–287.

Chandy, K. G. 1991. Simplified gene nomenclature. *Nature.* 352:26.

Cukierman, S., W. C. Zinkand, R. J. French, and B. K. Krueger. 1988. Effects of membrane surface charge and calcium on the gating of rat brain sodium channels in planar bilayers. *J. Gen. Physiol.* 92:431–447.

Dubois, J. M. 1981. Evidence for the existence of three types of potassium channels in the frog Ranvier node membrane. *J. Physiol.* 318:297–316.

Durell, S. R., and H. R. Guy. 1992. Atomic scale structure and functional models of voltage-gated potassium channels. *Biophys. J.* 62:238–250.

Elinder, F., and P. Århem. 1993. The surface charge of different K channels: a comparison between estimations from electrophysiology and primary structures. *In* Molecular Bases of ion channel function. R. W. Aldrich and J. López-Barneo, editors. Instituto Juan March de Estudios e Investigaciones, Madrid. 80–81.

Elinder, F., and P. Århem. 1994. Effects of gadolinium on ion channels in the myelinated axon of *Xenopus laevis*. *Biophys. J.* 67:71–83.

Evans, C. H. 1990. Biochemistry of the Lanthanides. Plenum Press, New York 444 pp.

Frankenhaeuser, B., K. Ryan, and P. Århem. 1976. The effects of neuraminidase and protamine chloride on potential clamp parameters of the node of Ranvier. *Acta Physiol. Scand.* 96:548–557.

Frech, G. C., A. M. J. VanDongen, G. Schuster, A. M. Brown, and R. H. Joho. 1989. A novel potassium channel with delayed rectifier properties isolated from rat brain by expression cloning. *Nature.* 340:642–645.

Glasstone, S., K. J. Laidler, and H. Eyring. 1941. The Theory of Rate Processes. McGraw-Hill, New York, 611 pp.

Grahame, D. C. 1947. The electrical double layer and the theory of electrocapillarity. *Chem. Rev.* 41:441–501.

Green, W. N., L. B. Weiss, and O. S. Andersen. 1987. Batrachotoxin-modified sodium channels in planar lipid bilayers. *J. Gen. Physiol.* 89: 841–872.

Grupe, A., K. H. Schröter, J. P. Ruppersberg, M. Stocker, T. Drewes, S. Beckh, and O. Pongs. 1990. Cloning and expression of a human voltage-gated potassium channel. A novel member of the RCK potassium channel family. *EMBO J.* 9:1749–1756.

Guy, H. R., and F. Conti. 1990. Pursuing the structure and function of voltage-gated channels. *Trends Neurosci.* 13:201–206.

Hille, B., A. M. Woodhull, and B. I. Shapiro. 1975. Negative surface charge near sodium channels of nerve: divalent ions, monovalent ions, and pH. *Philos. Trans. R. Soc. Lond. B. Biol. Sci.* 270:301–318.

Hwang, P. M., C. E. Glatt, D. S. Bredt, G. Yellen, and S. H. Snyder. 1992. A novel K^+ channel with unique localizations in mammalian brain: molecular cloning and characterization. *Neuron.* 8:473–481.

Jonas, P., M. Knopf, D. S. Koh, W. Kues, J. P. Ruppersberg, W. Vogel. 1992. Molecular basis of the diversity of voltage-dependent K channels in the peripheral and central nervous system. *Pfügers Arch.* 420:R30.

Kayano, T., M. Noda, V. Flockerzi, H. Takahashi, and S. Numa. 1988. Primary structure of rat brain sodium channel III deduced from cDNA sequence. *FEBS Lett.* 228:187–194.

McLaughlin, S. 1989. The electrostatic properties of membranes. *Annu. Rev. Biophys. Biophys. Chem.* 18:113–36.

Miller, C. 1991. 1990: annus mirabilis of potassium channels. *Science.* 252: 1092–1096.

Miller, C. 1992. Hunting for the pore of voltage-gated channels. *Curr. Biol.* 2:573–575.

Noda, M., T. Ikeda, T. Kayano, H. Suzuki, H. Takeshima, M. Kurasaki, H. Takahashi, and S. Numa. 1986. Existence of distinct sodium channel messenger RNAs in rat brain. *Nature.* 320:188–192.

Numann, R., W. A. Catterall, and T. Scheuer. 1991. Functional modulation of brain sodium channels by protein kinase C phosphorylation. *Science.* 254:115–118.

Ohmori, H., and M. Yoshii. 1977. Surface potential reflected in both gating and permeation mechanisms of sodium and calcium channels of the tunicate egg cell membrane. *J. Physiol.* 267:429–463.

Papazian, D. M., L. C. Timpe, Y. N. Jan, and L. Y. Jan. 1991. Alteration of voltage-dependence of *Shaker* potassium channel by mutations in the S4 sequence. *Nature.* 349:305–310.

Pongs, O. 1992. Molecular biology of voltage-dependent potassium channels. *Physiol. Rev.* 72:S69–S88.

Pusch, M. 1990. Divalent cations as probes for structure-function relationships of cloned voltage-dependent sodium channels. *Eur. Biophys. J.* 18:327–333.

Recio-Pinto, E., W. Thornhill, D. S. Duch, S. R. Levinson, and B. W. Urban. 1990. Neuroaminidase treatment modifies the function of electroplax sodium channels in planar lipid bilayers. *Neuron.* 5:675–684.

Rettig, J., F. Wunder, M. Stocker, R. Lichtinghagen, F. Mastiaux, S. Beckh, W. Kues, P. Pedarzani, K. H. Schröter, J. P. Ruppersberg, R. Veh, and O. Pongs. 1992. Characterization of a Shaw-related potassium channel family in rat brain. *EMBO J.* 11:2473–2486.

Safronov, B. V., K. Kampe, and W. Vogel. 1993. Single voltage-dependent potassium channels in rat peripheral nerve membrane. *J. Physiol.* 460: 675–691.

Sammar, M., G. Spira, and H. Meiri. 1992. Depolarization exposes the voltage sensor of the sodium channels to the extracellular region. *J. Membr. Biol.* 125:1–11.

Spires, S., and T. Begenisich. 1992a. Modification of potassium channel kinetics by amino group reagent. *J. Gen. Physiol.* 99:109–129.

Spires, S., and T. Begenisich. 1992b. Chemical properties of the divalent cation binding site on potassium channels. *J. Gen. Physiol.* 100:181–193.

Stevens, C. F. 1991. Making a submicroscopic hole in one. *Nature.* 349:657.

Stühmer, W., J. P. Ruppersberg, K. H. Schröter, B. Sakmann, M. Stocker, K. P. Giese, A. Perschke, A. Baumann, and O. Pongs. 1989. Molecular basis of functional diversity of voltage-gated potassium channels in mammalin brain. *EMBO J.* 8:3235–3244.

Terlau, H., S. H. Heinemann, W. Stühmer, M. Pusch, F. Conti, K. Imoto, and S. Numa. 1991. Mapping the site of block by tetrodotoxin and saxitoxin of sodium channel II. *FEBS Lett.* 293:93–96.

Trimmer, J. S., S. S. Cooperman, S. A. Tomiko, J. Zhou, S. M. Crean, M. B. Boyle, R. G. Kallen, Z. Sheng, R. L. Barchi, F. J. Sigworth, R. H. Goodman, W. S. Agnew, and G. Mandel. 1989. Primary structure and functional expression of a mammalian skeletal muscle sodium channel. *Neuron.* 3:33–49.

Westenbroek, R. E., D. K. Merrick, and W. A. Catterall. 1989. Differential subcellular localization of the R_I and R_{II} Na^+ channel subtypes in central neurons. *Neuron.* 3:695–704.

Worley, J. F., R. J. French, B. A. Pailthorpe, and B. K. Krueger. 1992. Lipid surface charge does not influence conductance or calcium block of single sodium channels in planar bilayers. *Biophys. J.* 61:1353–1363.